ASM Handbook, Volume 11: Failure Analysis and Prevention
W.T. Becker, R.J. Shipley, editors, p243-249
DOI: 10.31399/asm.hb.v11.a0003513

Failure Assessment Diagrams

Harold S. Reemsnyder, Fracture Technology Associates

OPTIMIZED MODELING of fracture-critical structural components and connections requires the application of elastic-plastic fracture mechanics. Such applications, however, can require sophisticated analytical techniques that require time and/or resources beyond those available to the designer or analyst. One of the first engineering tools to address this dilemma was The Welding Institute dimensionless crack tip opening displacement (CTOD), design curve (Ref 1), which was included in the first edition of the British Standards Institution (BSI) fitness-for-purpose guidance PD 6493 (Ref 2). The engineering tool receiving attention currently is the failure assessment diagram (FAD). This approach has been used primarily in the electric power industry both in Great Britain as the R6 criteria (Ref 3) and in the United States as both the FAD (Ref 4) and the deformation plasticity failure assessment diagram (DPFAD) (Ref 5). Both the R6 and DPFAD approaches use the *J*-integral criteria for fracture-driving force and resistance (i.e., toughness). The second edition of the BSI PD 6493 (Ref 6) presents failure assessments in the form of FADs using CTOD to characterize both crack-driving force and fracture toughness. The British Standards Institution has issued an updated and expanded version of PD 6493 as BS 7910 (Ref 7). In addition, the FAD is the recommended approach for the damage-tolerance analysis of ship structures (Ref 8). The background and derivations of the FAD were the subject of a theme issue of *The International Journal of Pressure Vessels and Piping* (Ref 9). Applications of, and experience with, the FAD concept were discussed in a seminar held by the Institution of Mechanical Engineers (Ref 10).

Origin and Description of the Failure Assessment Diagram

The United Kingdom Central Electricity Generating Board (CEGB) first proposed a failure assessment diagram (Fig. 1) based on the two-criteria approach of Dowling and Townley (Ref 11). The CEGB approach (Ref 3,12,13) addressed post-yield fracture by an interpolation formula between two limiting cases: linear elastic fracture and plastic collapse. The interpolation formula, known as the *failure assessment* or *R6 curve* (Fig. 1), developed from the Dugdale solution for a cracked, infinite plate, is:

$$K_r = \frac{S_r}{\sqrt{\frac{8}{\pi^2}\cdot \ln\left[\sec\left(0.5\cdot\pi\cdot S_r\right)\right]}} \quad \text{(Eq 1)}$$

The right-hand side of Eq 1 may be viewed as the plastic correction to the small-scale yielding prediction. In Eq 1, the fracture ratio K_r is:

$$K_r = \frac{K_I}{K_{mat}} \quad \text{(Eq 2)}$$

and the collapse ratio S_r is:

$$S_r = \frac{\sigma}{\sigma_c} \quad \text{(Eq 3)}$$

In Eq 2, K_I is the stress-intensity factor (a function of nominal stress σ, crack size *a*, and geometry) at fracture of the component, and K_{mat} is the linear elastic fracture toughness of the component. (K_{mat}, the linear elastic fracture toughness, is the value of K_I at fracture and, for a given material condition, is a function of thickness and temperature. The lower bound to K_{mat}, for a given temperature, is the plane-strain fracture toughness K_{Ic}.) In Eq 3, σ is the applied (remote) stress in the component at fracture and σ_c is the applied (remote) stress at plastic collapse of the cracked component.

If a point describing the state of a component or structure (e.g., point *W*) falls below the R6 curve (Fig. 1), the structure is considered to be *safe*. A point falling on or above the R6 curve represents *failure*. If a ray were constructed from the origin *O* through point *W* to the R6 curve (i.e, point F), the safety factor on load is the length of the ray from the origin to the intersection of the ray and the R6 curve divided by the length of the ray from the origin to point *W* (e.g., *OF*/*OW*). One application of the R6 curve is shown in Fig. 1 for a center-cracked panel with the crack size 20% of the panel width *W* and the applied stress σ 25% of the yield stress σ_y. In Fig. 1, the safety factor on load is *OF*/*OW* = 2.5.

The FAD as generally used today is, essentially, a graphical model, shown schematically in Fig. 2, that reflects the stress-strain curve of the material. The FAD consists of two elements: the failure assessment curve (FAC) and the failure assessment point (FAP). The collapse ratio, S_r or L_r, is the ratio of the applied stress at design load to the applied stress at plastic collapse. (S_r is a function of flow stress, σ_f, which is the average of the yield and tensile strengths, respectively,

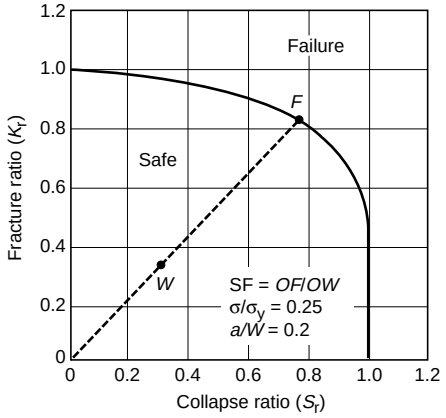

Fig. 1 Failure assessment diagram (R6 curve) as proposed by the United Kingdom Central Electricity Generating Board. SF, safety factor; σ, applied stress; σ_y, yield strength; a, crack length; W, panel width

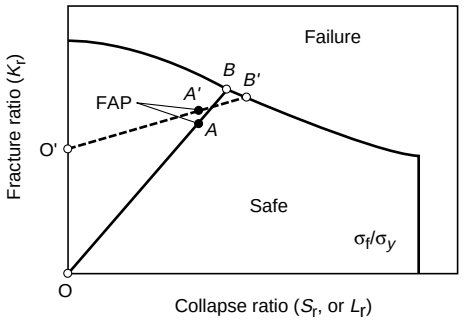

Fig. 2 Example of a typical failure assessment diagram. FAP, failure assessment point; FAC, failure assessment curve; σ_f, flow strength, average of yield and tensile strengths; σ_y, yield strength; solid line, without residual stress; dashed line, with residual stress

σ_y and σ_u; L_r is a function of yield stress.) K_r, the fracture ratio, is the ratio of the crack-driving force (including residual stress when applicable) to the material toughness (expressed as K_I, J-integral, or CTOD, δ). The FAC defines the critical combination of service loads, material stress-strain properties, and geometry of the cracked member at which failure might be expected. The FAP defines the state of a member containing a flaw of given size under specific service loads. The factor of safety (on load) against failure for a given FAP (in the absence of residual stresses) is the ratio of the line segments *OB*/*OA* (Fig. 2). In Fig. 2, it is observed that, in the presence of residual stresses, the factor of safety is reduced (i.e., $O'B'/O'A'$ is less than *OB*/*OA*).

Current applications of this form of the FAD are: CEGB R6, Revision 3 (Ref 3), BS 7910 (Ref 7), EPRI/GE model (Ref 4), deformation plasticity FAD (Ref 5), ASME Section XI Code Case (DPFAD) for ferritic piping (Ref 14), and damage-tolerance analysis of ship structures (Ref 8).

Current R6 Failure Assessment Diagrams

Chell (Ref 15) and Bloom (Ref 16) pointed out that K_r (Eq 1) could be interpreted as a ratio of J-integrals:

$$K_r = \sqrt{\frac{J_e}{J}} = f(S_r) \qquad \text{(Eq 4)}$$

where J_e, the elastic component of total J-integral J, is:

$$J_e = \frac{K_I^2}{E} \cdot (1 - \nu^2) \qquad \text{(Eq 5)}$$

where E is Young's modulus and ν is Poisson's ratio.

The current version of the R6 FAD (Ref 3, 12, 13) expresses K_r as a ratio of the linear elastic stress-intensity factor associated with the stress and the flaw to the J-integral toughness. Further, the current R6 presents three options for the FAC and three analysis categories for the FAP.

Option 1 FAC is recommended for materials with a low initial work-hardening rate, or as an initial screening test, or when details of the material stress-strain curve are not known. Option 1 is not recommended for materials with discontinuous stress-strain curves. The Option 1 FAC is an empirical fit to option 2 FACs for a variety of steels (including an elastic-perfectly plastic material) but biased toward a lower bound (Ref 9).

Option 2 FAC is recommended for materials with a high initial work-hardening rate, (e.g., strain-aging mild steels), or for materials with a discontinuous yield point, or when the complete material true stress-strain curve is known. The Option 2 FAC was developed from expressions for J-integrals from the EPRI/GE handbook (Ref 4) reformulated to use actual true stress-strain curves. Also, approximations erring on the conservative side were introduced to make the formulae geometrically independent, thus obviating the need for fully plastic power-law solutions for each geometry (Ref 9).

Option 3 FAC is the most sophisticated of the three options and requires a J-integral R-curve for the subject material. (An R-curve is a plot of the crack driving force (K_I, J, or CTOD δ) versus stable crack extension under monotonic, increasing load. Stable crack extension ceases when the loading rate goes to zero.) Option 3 acknowledges the presence of stable crack extension and a concomitant increase in fracture toughness. The construction of the Option 3 FAC is identical to that of the EPRI/GE FAD (Ref 4) and Bloom's DPFAD (Ref 5). Also, Appendix 8, R6, Revision 3, presents an FAC for C-Mn steels. The Appendix 8 FAC is an empirical lower bound to R6 Option 1 FACs for a variety of C-Mn steel plates and weld metal, finite element J-analyses (R6 Option 3), and tests on center-cracked panels and compact tension specimens (Ref 9). In Options 1, 2, and 3, the collapse ratio is expressed as L_r, while Appendix 8 uses S_r to represent the same.

Analysis Categories. Analysis Category 1 acknowledges elastic-plastic interaction of applied and residual stresses in the computation of K_I. Category 2 consists of two FAPs—one using a_0 and one using $a_0 + \Delta a_g$ where Δa_g is the maximum stable crack extension permitted in a J-integral fracture toughness test. Category 3 consists of several FAPs computed using various amounts of stable crack extension Δa as in the EPRI/GE FAD (Ref 4) and the DPFAD (Ref 5). The plastic-collapse load formulae used to compute L_r for the FAP are reviewed in Ref 9.

Table 1 Characterizations of elastic-plastic fracture toughness

Final event	Location on toughness-temperature curve	Significant stable crack extension	J-integral toughness, J_{mat}	CTOD toughness, δ_{mat}
Unstable fracture or onset of pop-in	Lower shelf	No	J_c	δ_c
Unstable fracture or onset of pop-in	Transition	Yes	J_u	δ_u
First attainment of maximum load plateau	Upper shelf	Yes	J_m	δ_m

J_{mat}, general J-integral fracture toughness of material; CTOD, crack-tip opening displacement; δ_{mat}, general CTOD toughness of material; J_c, J-integral fracture toughness, no significant stable crack extension, unstable fracture; δ_c, CTOD fracture toughness, no significant stable crack extension, unstable fracture; J_u, J-integral fracture toughness, significant stable crack extension, unstable fracture; δ_u, CTOD fracture toughness, significant stable crack extension, unstable fracture; J_m, J-integral fracture toughness, significant stable crack extension, plastic collapse; δ_m, CTOD fracture toughness, significant stable crack extension, plastic collapse

Current Fracture Criteria of BS 7910

BS 7910 (Ref 7), the successor to PD 6493 (Ref 6), incorporates a three-tiered (or 3-level) FAD criterion using CTOD as the characterization of both crack-driving force and fracture toughness.

The tiered approach to the FAD treats the problem with increasing analytical sophistication and data requirements and decreasing conservatism. The first tier or level (the least sophisticated and the most conservative) requires only an elastic fracture mechanics analysis and uses single-value estimates of fracture toughness (e.g., δ_c, δ_u, or δ_m) (Table 1).

On the other hand, the highest tier (the most sophisticated and least conservative) requires an elastic-plastic fracture mechanics analysis and uses the tearing resistance of the material (J or CTOD R-curve). In addition, the highest tier requires the expression of the true stress-strain curve of the material. The procedure is to evaluate a given situation at the first tier, and if the FAP falls below the FAC, safe performance is concluded. If, however, the FAP falls on or above the FAC, then the investigator goes to the second tier analysis and so on. If an unsafe situation is predicted at the highest tier, a redesign or selection of a tougher material is required.

Level 1 FAC (Fig. 3), a recasting of the dimensionless CTOD design curve (Ref 1) (based on wide-plate fracture tests), may be thought of as a screening method and includes a safety factor of approximately 2 on flaw size in the construction of the FAC. For the FAP (not shown in Fig. 3), K_r is the square root of the ratio of the applied elastic CTOD δ_e to the material CTOD toughness δ_{mat} or

$$K_r = \sqrt{\frac{\delta_e}{\delta_{mat}}} \qquad \text{(Eq 6)}$$

The elastic CTOD δ_e, for steels (including stainless steels) and aluminum alloys, is determined from the elastic stress-intensity factor K_I con-

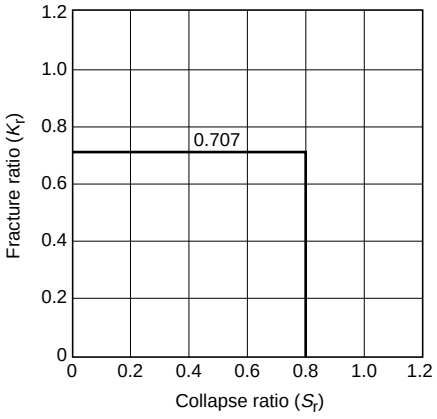

Fig. 3 Level 1 failure assessment diagram (BS 7910)

comitant with σ_{max}, the sum of the applied and residual stresses:

$$\delta_e = \frac{K_I^2}{\sigma_y \cdot E} \text{ for } \frac{\sigma_{max}}{\sigma_y} \le 0.5 \quad \text{(Eq 7)}$$

or

$$\delta_e = \frac{K_I^2}{\sigma_y \cdot E}\left(\frac{\sigma_y}{\sigma_{max}}\right)\left(\frac{\sigma_{max}}{\sigma_y} - 0.25\right) \text{ for } \frac{\sigma_{max}}{\sigma_y} > 0.5 \quad \text{(Eq 8)}$$

No elastic-plastic interaction of applied and residual stresses is acknowledged in the computation of K_r (i.e., the validity of superposition is assumed). The material CTOD toughness δ_{mat} is the fracture-test-estimated value δ_c, δ_u, or δ_m (Ref 17, 18).

S_r is the ratio of the effective net-section stress σ_{ref} to the flow stress:

$$S_r = \frac{\sigma_{ref}}{\sigma_f} \quad \text{(Eq 9)}$$

(The effective net-section stress σ_{ref} is the net-section stress computed in such a way that S_r is equivalent to the ratio of the applied (remote) stress to the applied (remote) stress at plastic collapse [Ref 7, 19, 20].)

Level 2a FAC (Fig. 4) is meant for low work-hardening materials and is identical to the original form of the R6 curve (Eq 1) based on Dugdale's strip-yield model and is expressed as an inverse function of the log-secant of L_r.

$$K_r = \frac{L_r \cdot \sigma_y / \sigma_f}{\sqrt{\frac{8}{\pi^2} \cdot \ln\left[\sec\left(\frac{\pi \cdot \sigma_y}{2 \cdot \sigma_f} \cdot L_r\right)\right]}} \quad \text{(Eq 10)}$$

L_r in Eq 10 is the ratio of the effective net-section stress σ_{ref} to the yield stress:

$$L_r = \frac{\sigma_{ref}}{\sigma_y} \quad \text{(Eq 11)}$$

The expression for the coordinate K_r of the FAP (not shown in Fig. 4) includes a constraint factor X and acknowledges the inelastic stress redistribution due to the interaction of the applied and residual stresses through the plasticity correction factor ρ (in the manner of the present R6 approach). K_r is expressed as:

$$K_r = \sqrt{\frac{\delta_e}{\delta_{mat}}} + \rho \quad \text{(Eq 12)}$$

where

$$\delta_e = \frac{K_I^2}{X \cdot \sigma_y \cdot E'} \quad \text{(Eq 13)}$$

For plane stress and low work-hardening materials, X and E' are, respectively, 1 and E, while for plane strain and low work-hardening materials, X and E' are, respectively, 2 and $E/(1 - \nu^2)$. X is affected by work hardening and can be determined from either elastic-plastic analyses or fracture toughness tests:

$$X = \frac{J_{mat}}{\sigma_y \cdot \delta_{mat}} \quad \text{(Eq 14)}$$

The plasticity correction factor ρ to accommodate residual stresses is determined by:

$$\begin{aligned} \rho &= \rho_1 && \text{for} \quad L_r \le 0.8 \\ \rho &= 4 \cdot \rho_1 \cdot (1.05 - L_r) && \text{for} \quad 0.8 < L_r < 1.05 \\ \rho &= 0 && \text{for} \quad L_r \ge 1.05 \end{aligned} \quad \text{(Eq 15)}$$

where

$$\begin{aligned} \rho_1 &= 0 && \text{for} \quad \chi \le 0 \\ \rho_1 &= 0.1 \cdot \chi^{0.714} - 0.007 \cdot \chi^2 - 3x10^{-5} \cdot \chi^5 && \text{for} \quad 0 < \chi < 5.2 \\ \rho_1 &= 0.25 && \text{for} \quad \chi \ge 5.2 \end{aligned} \quad \text{(Eq 16)}$$

In Eq 16, χ is:

$$\chi = \frac{K_I^{residual}}{K_I^{applied}} \cdot L_r \quad \text{(Eq 17)}$$

where $K_I^{applied}$ and $K_I^{residual}$ are the linear elastic stress-intensity factors for, respectively, the applied and residual stresses. Equations 15 and 16 are applicable when χ is less than or equal to 4. When χ exceeds 4, a more detailed procedure for the computation of ρ is presented in Ref 7.

There is *no* safety factor inherent to the Level 2a FAC, and the latter should be considered critical in the assessment. It is believed that Level 2a is the preferred method for most cases. However, the Level 2a model of the FAC is inaccurate for high work-hardening materials.

Levels 2b and 2c (Fig. 5) generally are used in the assessment of high work-hardening materials and/or stable tearing where the Level 2a approach would prove too restrictive.

Level 2b (Fig. 5) is a general FAC similar to Option 1 of the current R6 method (Ref 3) and is expressed as:

$$K_r = \left(1 - 0.14 \cdot L_r^2\right) \cdot \left[0.3 + 0.7 \cdot \exp\left(-0.65 \cdot L_r^6\right)\right] \text{ for } L_r \le L_r^{max} \quad \text{(Eq 18)}$$

or

$$K_r = 0 \text{ for } L_r > L_r^{max} \quad \text{(Eq 19)}$$

where L_r is defined by Eq 11 and L_r^{max} is defined as:

$$L_r^{max} = \frac{\sigma_f}{\sigma_y} \quad \text{(Eq 20)}$$

Level 2b may be used for all cases but is recommended (Ref 7) for high work-hardening materials (i.e., when $\sigma_f > 1.2\ \sigma_y$).

Level 2c (Fig. 5), a material-specific FAC similar to Option 2 of the current R6 (Ref 3), is suitable for base and weld metal of all types and provides more accurate results than either Level 2a or 2b but requires the stress-strain curve for the material examined. Level 2c FAC is expressed as:

$$K_r \frac{1}{\sqrt{\frac{E \cdot \varepsilon}{L_r \cdot \sigma_y} + \frac{L_r^3 \cdot \sigma_y}{2 \cdot E \cdot \varepsilon}}} \text{ for } L_r \le L_r^{max} \quad \text{(Eq 21)}$$

and

$$K_r = 0 \text{ for } L_r > L_r^{max} \quad \text{(Eq 22)}$$

where L_r is expressed by Eq 11, L_r^{max} is expressed by Eq 20, and ε is the true strain for a true stress of $L_r\ \sigma_y$ from the true stress-strain curve of the material.

The coordinate L_r (Fig 5) is the ratio of the net-section stress to the yield stress σ_y. Inelastic stress redistribution due to the interaction of the applied and residual stresses is handled as in Level 2b.

K_r for the general FAC is a function only of L_r, and for the material specific FAC, is a func-

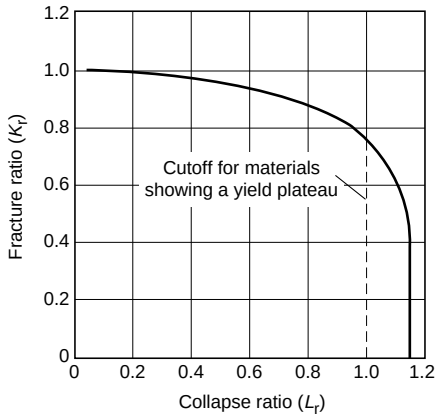

Fig. 4 Level 2a failure assessment diagram (BS 7910)

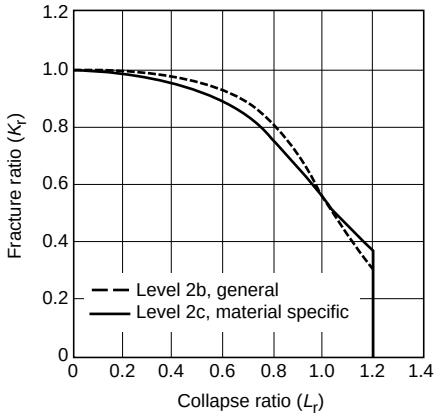

Fig. 5 Level 2b and level 2c failure assessment diagram (BS 7910)

tion of L_r, yield strength σ_y, and the true stress-strain curve. K_r for the FAP is identical in form to that of Level 2a in Eq 12. Residual stresses are accommodated in Levels 2b and 2c as in Level 2a (i.e., Eq 15, 16, and 17). There is no safety factor inherent to either Level 2b or 2c FAC, and they should be considered critical in the assessment.

It should be noted that, as in Levels 1 and 2a, only the elastic stress-intensity factor K_I for the flawed member is needed.

Level 2c FACs for two materials with identical yield and tensile strengths, respectively, σ_y and σ_u (Fig. 6), are compared with the Level 2b (general FAC) in Fig. 7. Both stress-strain curves were developed from tension tests on an HSLA 60 steel (API 2Y grade 60T, a plate steel used in offshore welded construction) base metal (showing a yield plateau in Fig. 6) and the deposited weld metal (showing a roundhouse in Fig. 6) in the same steel. Below an L_r of 0.6, there is little difference between the Level 2b and Level 2c FACs, (Fig. 7). However, for L_r greater than 0.6, the effect of stress-strain-curve shape is marked. Note that in Fig. 6 and 7, the base metal and deposited weld metal are represented by, respectively, the solid and dashed curves.

Level 3 FADs include a ductile tearing assessment. Levels 3a and 3b apply ductile tearing assessments to, respectively, the FAD of Level 2a or 2b, and to the FAD of Level 2c. Level 3c uses the *J*-integral in a tearing assessment similar to R6 Option 3 (Ref 3) or the EPRI/GE handbook (Ref 4). Such an analysis requires the *J*-integral solutions for any geometry. The complete solutions for many geometries are listed in the EPRI/GE handbook (Ref 4), subsequent EPRI/GE reports (Ref 21, 22, 23), and the textbook by Kanninen and Popelar (Ref 12). EPRI and Novetech jointly developed the three-volume *Ductile Fracture Handbook* (Ref 24) that assembled and synthesized the elastic-plastic fracture mechanics solutions for cracked cylinders developed in EPRI-sponsored research. The first volume of the *Ductile Fracture Handbook* presents solutions for circumferential through-wall cracks. The second volume presents solutions for circumferential part-through-wall cracks and axial through-wall cracks. The third volume presents solutions for axial part-through-wall cracks and cracks in elbows, tees, and nozzles and flaw-evaluation procedures for piping and pressure vessels.

Table 2 Fracture ratios, K_r

FAD element	LEFM	EPFM	
		J-integral	CTOD
FAC	1	$\sqrt{\frac{J_e}{J_e + J_p}}$	$\sqrt{\frac{\delta_e}{\delta_e + \delta_p}}$
FAP	$\frac{K_I}{K_{mat}}$	$\sqrt{\frac{J_e}{J_{mat}}}$	$\sqrt{\frac{\delta_e}{\delta_{mat}}}$

FAD, failure assessment diagram; LEFM, linear elastic fracture mechanics; EPFM, elastic-plastic fracture mechanics; CTOD, crack-tip opening displacement; FAC, failure assessment curve; FAP, failure assessment point; J_e, elastic component of *J*-integral; J_p, plastic component of *J*-integral; δ_e, elastic component of crack-tip opening displacement; δ_p, plastic component of crack-tip opening displacement; K_I, mode I stress-intensity factor; K_{mat}, general linear elastic fracture toughness of material; J_{mat}, general *J*-integral fracture toughness of material; δ_{mat}, general CTOD toughness of material

Considerations in Use

The characterizations for the fracture ratio K_r of the FAD are shown in Table 2 for linear elastic fracture mechanics (LEFM) and elastic-plastic fracture mechanics (EPFM). It is vital to recognize that the FAD acknowledges elastic-plastic response both in the fracture event and plastic collapse. Also, only the linear elastic stress-intensity factor K_I for a specific geometry is required, thus using the existing compendia of K_I solutions and obviating the need for complex elastic-plastic solutions. However, application of the FAD does require the knowledge of the elastic-plastic fracture toughness (characterized as either *J*-integral or CTOD) for the material in the thickness of application.

Also, R6 (Ref 3) and BS 7910 (Ref 7) give guidance on reliability, partial safety factors, number of fracture toughness tests, selection of failure risk for Levels 2 and 3, and sensitivity analyses.

Limitations to be addressed in the future include the improvement of estimates of material toughness through:

- The evaluation of constraint
- Improved estimation equations for *J*-integral and CTOD from test results
- Use of shallow cracks more typical of service

Improvements in the construction of the FAD include:

- Combining the applied and residual stresses to acknowledge inelastic redistribution of residual stresses
- Consideration in mismatch between the mechanical properties of the base metal and deposited weld metal
- Ductile tearing (Level 3, PD 7910) beyond that allowed by the validity criteria of current fracture toughness test standards
- Consideration of constraint in the definition of the FAC and FAP

Caution. Many practitioners of fracture mechanics today determine the critical stress-crack-size $K_I^{critical}$ from the test estimations of elastic-plastic fracture toughness (i.e., J_{mat} or δ_{mat}) (Table 1) through:

$$K_I^{critical} = \sqrt{\frac{J_{mat} \cdot E}{(1 - \nu^2)}} \quad \text{(Eq 23)}$$

or

$$K_I^{critical} = \sqrt{\delta_{mat} \cdot E \cdot \sigma_y} \quad \text{(Eq 24)}$$

Such an approach implies that $K_r = 1$ regardless of the value of L_r (Fig. 8). In Fig. 8, it may be seen that K_r, equivalent to $\sqrt{\delta_e / \delta_{mat}}$ (Table 2), can be significantly less than 1, depending on the value of L_r. The observed ratios of $\sqrt{\delta_e / \delta_{mat}}$ versus the test-estimated CTOD toughness for an HSLA 50 steel (API 2Y Grade 50T, a plate steel

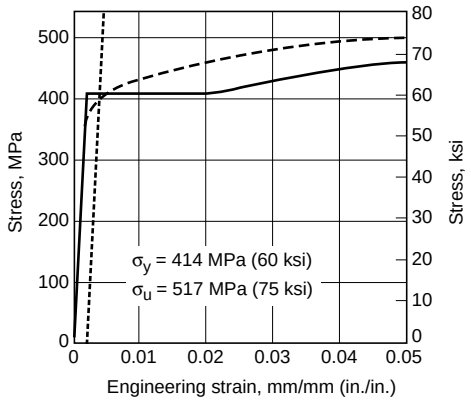

Fig. 6 Engineering stress-strain curve for HSLA 60 (API 2Y grade 60T) plate steel. σ_y, yield strength; σ_u, tensile strength

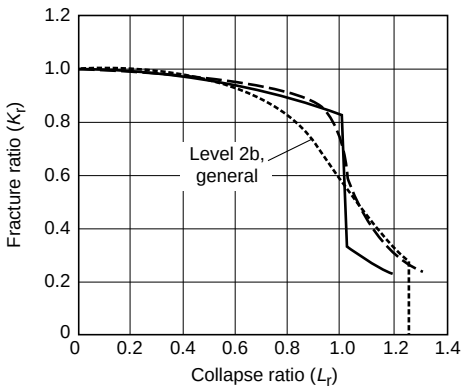

Fig. 7 Level 2b and 2c failure assessment diagram for HSLA 60 (API 2Y grade 60T) plate steel

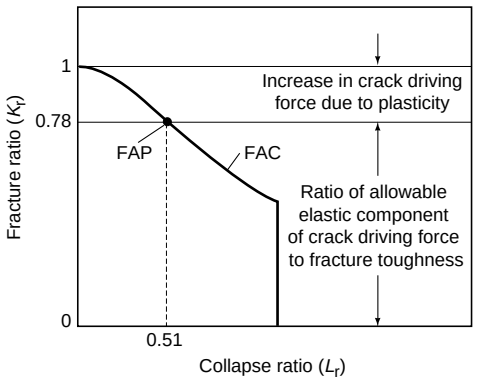

Fig. 8 Failure assessment diagram with $K_r < 1$, depending on the value of L_r. FAP, failure assessment point; FAC, failure assessment curve

used in offshore welded construction) are shown in Fig. 9. With the observed range of values δ_e/δ_{mat} for the various δ_{mat} (i.e., δ_c, δ_u, and δ_m, defined in Table 1), $K_I^{critical}$ may be computed through a combination of Eq 12, 13, and 24 (Table 3).

From Eq 24, the ratio $K_I^{critical}/\sqrt{\delta_{mat} \cdot \sigma_y \cdot E}$ would always be unity. However, recognition of elastic-plastic response at fracture, demonstrated by the FAD (e.g., Fig. 8) shows that the ratio $K_I^{critical}/\sqrt{\delta_{mat} \cdot \sigma_y \cdot E}$ can be significantly less than unity (Table 3). Obviously, the use of Eq 24 to estimate the critical stress–crack-length combination can be very unconservative.

Application Examples

Example 1: Application of FAD to determine the required CTOD toughness to develop the full potential for a transverse butt weld in a very wide 33 mm (1.3 in.) plate containing a surface flaw at the weld toe that penetrates the plate fully. Consider both the as-welded (AW) and postweld heat treated (PWHT) cases. The yield and tensile strengths are, respectively, σ_y = 414 MPa (60 ksi) and σ_u = 517 MPa (75 ksi). The applied stress σ_m is 331 MPA (48 ksi), or 80% of the yield strength. Assume that the residual stress σ_{resaw} transverse to the weld is equal to the yield stress. The residual stress after PWHT σ_{repwht} is 20% of that in the AW condition (Ref 7), or 82.8 MPA (12 ksi).

Hint: Estimate the fracture toughness when the FAP falls on the FAC for Levels 1 and 2, BS 7910 (Ref 7). Assume: (1) plane strain for Level 2, (2) the stress-strain curves for Level 2c are those shown in Fig. 6, and (3) the crack geometry is that of through-crack of length 2*a* in an infinitely wide plate of thickness *a*:

$$K_I = \sigma\sqrt{\pi \cdot a} \quad \text{(Eq 25)}$$

and

$$\sigma_{ref} = \sigma_m = 331 \text{ MPa (48 ksi)} \quad \text{(Eq 26)}$$

E, ν, and σ_f are, respectively, 206,897 MPa (30,000 ksi); 0.3; and 466 MPa (67.5 ksi). From Eq 9 and 11, the collapse ratios, S_r and L_r, are, respectively, 0.711 and 0.800.

Level 1, BS 7910. The maximum stresses for the AW and PWHT conditions are:

$$\sigma_{maxaw} = \sigma_m + \sigma_{resaw} = 745 \text{ MPa (108 ksi)} \quad \text{(Eq 27)}$$

$$\sigma_{maxpwht} = \sigma_m + \sigma_{respwht} = 414 \text{ MPa (60 ksi)} \quad \text{(Eq 28)}$$

and, from Eq 25, with $\sigma = \sigma_{maxaw}$ and $\sigma = \sigma_{maxpwht}$:

$$K_I^{maxaw} = 239 \text{ MPa}\sqrt{\text{m}}\left(217.5 \text{ ksi}\sqrt{\text{in.}}\right) \quad \text{(Eq 29)}$$

$$K_I^{maxpwht} = 133 \text{ MPa}\sqrt{\text{m}}\left(121.1 \text{ ksi}\sqrt{\text{in.}}\right) \quad \text{(Eq 30)}$$

From Fig. 3, K_r = 0.707, and from Eq 8, with $\sigma_{max}/\sigma_y > 0.5$:

$$\delta_I^{aw} = 0.323 \text{ mm (0.0127 in.)}$$
$$\delta_I^{pwht} = 0.156 \text{ mm (0.00613 in.)} \quad \text{(Eq 31)}$$

From Eq 6, for Level 1, the optimum fracture toughnesses are:

$$\delta_{mat}^{aw} = 0.643 \text{ mm (0.0253 in.)}$$
$$\delta_{mat}^{pwht} = 0.310 \text{ mm (0.0122 in.)} \quad \text{(Eq 32)}$$

Level 2a, BS 7910. The maximum stress-intensity factors, from Eq 25, for the AW and PWHT conditions are:

$$K_I^{aw} = K_I^m + K_I^{resaw} = \sigma_m \cdot \sqrt{\pi \cdot a} + \sigma_{resaw} \cdot \sqrt{\pi \cdot a} \quad \text{(Eq 33)}$$

$$K_I^{pwht} = K_I^m + K_I^{respwht} = \sigma_m \cdot \sqrt{\pi \cdot a} + \sigma_{respwht} \cdot \sqrt{\pi \cdot a} \quad \text{(Eq 34)}$$

and, from Eq 25, with $\sigma = \sigma_{maxaw}$ and $\sigma = \sigma_{maxwht}$:

$$K_I^{aw} = 239 \text{ MPa}\sqrt{\text{m}}\left(217.5 \text{ ksi}\sqrt{\text{in.}}\right) \quad \text{(Eq 35)}$$

$$K_I^{pwht} = 133 \text{ MPa}\sqrt{\text{m}}\left(121.1 \text{ ksi}\sqrt{\text{in.}}\right) \quad \text{(Eq 36)}$$

From Eq 10, K_r = 0.870, and from Eq 17:

$$\chi^{aw} = 1.00 \qquad \chi^{pwht} = 0.200 \quad \text{(Eq 37)}$$

From Eq 16, for $0 < \chi < 5.2$:

$$\rho_1^{aw} = 0.0930 \qquad \rho_1^{pwht} = 0.0314 \quad \text{(Eq 38)}$$

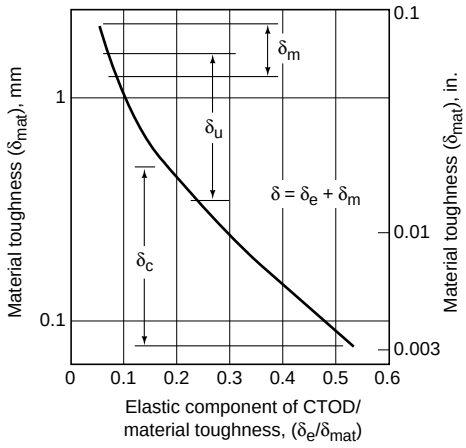

Fig. 9 Crack-tip opening displacement (CTOD) toughness, HSLA 50. δ, CTOD; δ_c, CTOD fracture toughness, no significant stable crack extension, unstable fracture; δ_e, elastic component of CTOD; δ_m, CTOD fracture toughness, significant stable crack extension, plastic collapse; δ_p, plastic component of CTOD; δ_u, CTOD fracture toughness, significant stable crack extension, unstable fracture

From Eq 15, for $L_r < 0.8$ (i.e., $\rho = \rho_1$):

$$\rho^{aw} = 0.0930 \qquad \rho^{pwht} = 0.0314 \quad \text{(Eq 39)}$$

From Eq 13, for plane strain with $X = 2$ and $E' = E/(1 - \nu^2)$:

$$\delta_I^{aw} = 0.305 \text{ mm (0.0120 in.)}$$
$$\delta_I^{pwht} = 0.0945 \text{ mm (0.00372 in.)} \quad \text{(Eq 40)}$$

For Level 2a, from:

$$\delta_{mat} = \frac{\delta_I}{(K_r - \rho)^2} \quad \text{(Eq 41)}$$

the optimum plane-strain fracture toughnesses are:

$$\delta_{mat}^{aw} = 0.508 \text{ mm (0.0200 in.)}$$
$$\delta_{mat}^{pwht} = 0.134 \text{ mm (0.00529 in.)} \quad \text{(Eq 42)}$$

Level 2b, BS 7910. The maximum stress-intensity factors, χ, ρ, and ρ_1, for the AW and PWHT conditions, are identical to those for Level 2a above. From Eq 18, K_r = 0.811. From Eq 13, for plane strain with $X = 2$ and $E' = E/(1 - \nu^2)$:

$$\delta_I^{aw} = 0.305 \text{ mm (0.0120 in.)}$$
$$\delta_I^{pwht} = 0.0945 \text{ mm (0.00372 in.)} \quad \text{(Eq 43)}$$

For Level 2b, from Eq 41, the optimum plane-strain fracture toughnesses are:

$$\delta_{mat}^{aw} = 0.594 \text{ mm (0.0234 in.)}$$
$$\delta_{mat}^{pwht} = 0.155 \text{ mm (0.00612 in.)} \quad \text{(Eq 44)}$$

Level 2c, BS 7910. The maximum stress-intensity factors, χ, ρ, and ρ_1, for the AW and PWHT conditions, are identical to those for Levels 2a and 2b above. The strain ε is computed from $\varepsilon = \sigma_m/E$ = 0.00160 (Fig. 6). From Eq 21, K_r = 0.870. From Eq 13, for plane strain with $X = 2$ and $E' = E/(1 - \nu^2)$:

$$\delta_I^{aw} = 0.305 \text{ mm (0.0120 in.)}$$
$$\delta_I^{pwht} = 0.0945 \text{ mm (0.00372 in.)} \quad \text{(Eq 45)}$$

Table 3 $K_I^{critical}$ from CTOD toughness

δ_{mat} (Table 1)	δ_e/δ_{mat} (Fig. 9)	$K_I^{critical}/\sqrt{\delta_{mat} \cdot \sigma_y \cdot E}$	
		Plane stress	Plane strain
δ_c	0.19–0.54	0.44–0.74	0.64–1.09
δ_u	0.07–0.23	0.26–0.48	0.39–0.71
δ_m	0.05–0.08	0.22–0.28	0.33–0.42

$K_I^{critical}$, mode I stress-intensity factor estimated from J_{mat} or δ_{mat}; CTOD, crack-tip opening displacement; δ_{mat}, general CTOD toughness of material; δ_e, elastic component of crack-tip opening displacement; σ_y, yield strength; *E*, Young's modulus; δ_c, CTOD fracture toughness, no significant stable crack extension, unstable fracture; δ_u, CTOD fracture toughness, significant stable crack extension, unstable fracture; δ_m, CTOD fracture toughness, significant stable crack extension, plastic collapse

For Level 2c, from Eq 41 the optimum plane-strain fracture toughnesses are:

$$\delta_{mat}^{aw} = 0.505 \text{ mm } (0.0199 \text{ in.})$$
$$\delta_{mat}^{pwht} = 0.134 \text{ mm } (0.00528 \text{ in.}) \quad \text{(Eq 46)}$$

The fracture toughnesses estimated from Levels 1, 2a, 2b, and 2c, BS 7910, are compared in Table 4. The toughnesses for Level 2c are slightly lower than those for Level 2b, which reflects the slight difference between the FAC for Level 2b and those of Level 2c (Fig. 7). The toughnesses for Levels 2a and 2c are practically identical. However, this is fortuitous because the values of K_r, for $L_r = 0.8$, are practically identical (Fig. 4, 7). If the stress-strain curves for the material demonstrated a greater strain-hardening effect than in Fig. 6, the fracture toughnesses for Level 2c would be greater than those of Level 2a. The fracture toughnesses required from the Level 1 analysis are 1.2 to 2.2 times those of the more accurate analysis of Level 2c, which reflects the conservative nature of Level 1. The decrease in required fracture toughness when PWHT is applied reflects only the reduction in residual stress that reduces the crack-driving force. The reader should remember that an improper PWHT could reduce the fracture toughness of the material.

Example 2: Application of FAD. The structural-integrity analysis of a heavy rolled W14 × 730 H-section (Fig. 10) used in high-rise building construction is presented in Ref. 25. Normally, such sections are used as columns in high-rise buildings, but in some cases, these sections are used as tension chords of trusses in such construction. The material fracture toughness, from tests on compact tension specimens taken from the flange-web core was linked to the estimation of the critical crack size in the section through an elastic-plastic structural-integrity analysis. The assessment methodology was that of the FAD. The fracture model for the section was assumed to be a surface flaw in one flange joined at the flange-web intersection to an edge flaw in the web (Fig. 10). The steel grade of the section was A 572 Grade 50, yield and tensile strengths of, respectively, 345 and 552 MPa (50 and 80 ksi). Crack-tip opening displacement toughness values δ_m (upper shelf, Table 1) of 0.25 to 0.76 mm (0.01 to 0.03 in.) estimated from the fracture toughness tests were used in the analysis. Both the presence and absence of rolling residual stresses were considered. (Maximum tensile residual stresses on the order of 69 MPa (10 ksi) were measured in the flange-web core.) Critical surface-flaw depths were estimated with and without residual stresses for a range of applied stresses S of 69 to 345 MPa (10 to 50 ksi) and for surface flaw aspect ratios a/c (Fig. 10) varying from 0.1 to 0.6. (Applied stress S is the applied load divided by the area of the uncracked cross section.) The fracture model for the cracked section was assumed to be a surface flaw in one flange joined at the web-flange intersection to an edge flaw in the web. Elastic continuity was established by matching the crack-mouth opening displacements (CMOD) of the two crack geometries at their junction. The crack depth a (Fig. 10) was varied from 19 to 83 mm (0.75 to 3.25 in.).

Three FAD approaches were used in the analyses:

- Level 2, PD 6493 (Ref 2), now Level 2a BS 7910 (Ref 7)
- Level 3 general, PD 6493, now Level 2b, BS 7910
- Appendix 8, R6, Revision 3, for C-Mn steels (Ref 3)

The results of the R6, Appendix 8, FAD analysis were the most conservative of the three approaches and are presented herein. The FAC for C-Mn steels from Appendix 8, R6, Revision 3 (Ref 3) is:

$$K_r = \frac{1 - 0.1 \cdot S_r^2 + 0.1 \cdot S_r^4}{1 + 3 \cdot S_r^4} \text{ for } S_r \le 1 \quad \text{(Eq 47)}$$

and

$$K_r = 0 \text{ for } S_r > 1 \quad \text{(Eq 48)}$$

where the fundamental definition of the collapse ratio S_r was used:

$$S_r = \frac{\text{applied load on cracked section}}{\text{limit load of cracked section}} \quad \text{(Eq 49)}$$

Solutions for an array of FAPs, (e.g., Fig. 11) were performed and resulted in an FAP surface for each aspect ratio a/c with nodes located at the intersections S, a (Fig. 11). In Fig. 11, two examples of FAP loci for one aspect ratio, $a/c = 0.5$, are shown: (1) $S = 138$ MPa (20 ksi), varying a from 19 to 82.6 mm (0.75 to 3.25 in), and (2) $a = 38.1$ mm (1.50 in), varying S from 69 to 345 MPa (10 to 50 ksi). The critical combination of S and a for each aspect ratio a/c is estimated from the intersection of the FAP surface with the FAC (Fig. 11). The results of this process are shown in Fig. 12 for one aspect ratio, $a/c = 0.5$, and the lower bound to the test-estimated upper-shelf CTOD toughness, $\delta_m = 0.25$ mm (0.010 in). Conclusions drawn for these analyses were (Ref 25):

- Typical surface flaws in flanges might be expected to have aspect ratios a/c on the order of 0.3 or greater. For such aspect ratios and values of applied stress typical of service, 138 to 207 MPa (20 to 30 ksi), the FAD analysis indicated that the minimum critical crack

Table 4 Optimum CTOD toughness mm (in.), at indicated level

Case	1	2a	2b	2c
AW	0.64 (0.025)	0.51 (0.020)	0.58 (0.023)	0.51 (0.020)
PWHT	0.31 (0.012)	0.13 (0.0053)	0.16 (0.0061)	0.13 (0.0053)

CTOD, crack-tip opening displacement; AW, as welded; PWHT, postweld heat treatment

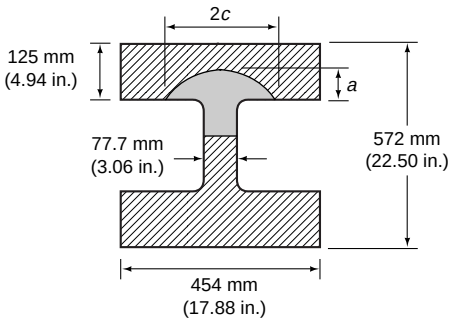

Fig. 10 W14 × 730 column H-section with assumed crack shape, a, depth of surface crack; $2c$, length of surface crack

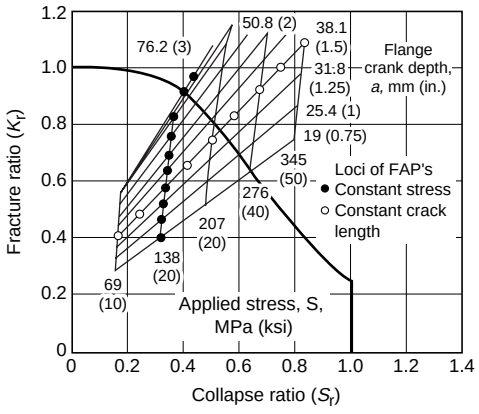

Fig. 11 Failure assessment diagram (R6, Appendix 8) for WF14 × 730 H-section, $a/c = 0.5$, with residual stresses. Collapse ratio is a function of flow stress σ_f; FAP, failure assessment point

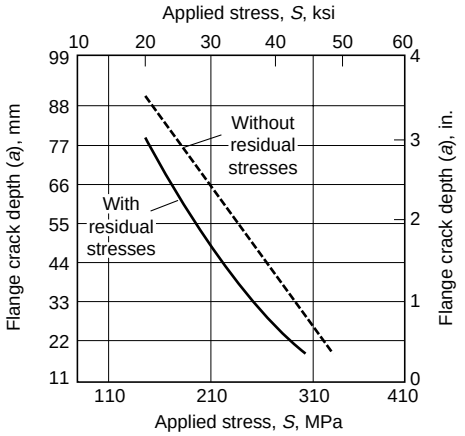

Fig. 12 Critical crack depth vs. applied stress for WF14 × 730 H-section, $a/c = 0.5$, $\delta_m = 0.25$ mm (0.010 in.)

depth *a* would be on the order of 38 to 51 mm (1.5 to 2 inches) (about 30 to 40% of the flange depth) when the upper shelf CTOD toughness δ_m was 0.25 mm (0.01 in).

- The critical flange crack depth would be increased by about 30 to 50% when the upper shelf CTOD toughness δ_m was increased from 0.25 mm (0.01 in.) to 0.76 mm (0.030 in.) (the upper bound from the fracture toughness tests).
- For an aspect ratio *a*/*c* of 0.5, CTOD toughness δ_m of 0.25 mm (0.01 in.), and applied stresses *S* from 138 to 207 MPa (20 to 30 ksi), the elimination of rolling residual stresses would increase the critical crack depth *a* by about 15 to 34%. (The rolling residual stresses would be reduced significantly by a thermal treatment, e.g., normalizing.)

Essentially, the analysis of this example was a sensitivity analysis (see Ref 3 and 7) to establish the effects on the structural integrity of the cracked H-section by variations in the significant parameters (e.g., applied stress *S*, crack depth *a*, surface-crack aspect ratio *a*/*c*, fracture toughness δ_m, and the presence or absence of residual stresses).

REFERENCES

1. F.M. Burdekin and M.G. Dawes, Practical Uses of Linear Elastic and Yielding Fracture Mechanics with Particular Reference to Pressure Vessels, *Practical Applications of Fracture Mechanics to Pressure Vessel Technology,* Institution of Mechanical Engineers, London, 1971, p 28–37
2. "Guidance on Some Methods for the Derivation of Acceptance Levels for Defects in Fusion Welded Joints," PD 6493:1980, 1st ed., British Standards Institution, London, March 1980
3. I. Milne, R.A. Ainsworth, A.R. Dowling, and A.T. Stewart, "Assessment of the Integrity of Structures Containing Defects," R/H/R6, Revision 3, Central Electricity Generating Board, Leatherhead, Surrey, May 1986
4. V. Kumar, M.D. German, and C.F. Shih, "An Engineering Approach for Elastic-Plastic Fracture Analysis," EPRI NP–1931, Project 1237-1, General Electric Company, Research and Development Center, Schenectady, NY, July 1981
5. J.M. Bloom, Validation of a Deformation Plasticity Failure Assessment Diagram Approach to Flaw Evaluation, *Elastic-Plastic Fracture: Second Symposium, Vol II, Fracture Resistance Curves and Engineering Applications,* STP 803, C.F. Shah and J.P. Gudas, Ed., ASTM, 1983, p II-206 to II-238
6. "Guidance on Methods for Assessing the Acceptability of Flaws in Fusion Welded Structures," PD 6493:1991, 2nd ed., British Standards Institution, London, August 1991
7. "Guidance on Methods for Assessing the Acceptability of Flaws in Fusion Welded Structures," BS 7910:1998, British Standards Institution, London, 1998
8. "Guide to Damage Tolerance Analysis of Marine Structures," SSC-409, Ship Structures Committee, Washington, DC, 2000
9. Theme Issue: The Revisions to the Structural Integrity Assessment Method CEGB/R6, *Int. J. Pressure Vessels Piping,* Vol 32, 1988
10. "20 Years of R6," S 458, Institution of Mechanical Engineers, London, Nov 1996
11. A.R. Dowling and C.H.A. Townley, The Effect of Defects on Structural Failure: A Two-Criteria Approach, *Int. J. Pressure Vessels Piping,* Vol 3, 1975, p 77–107
12. M.F. Kanninen and C.H. Popelar, *Advanced Fracture Mechanics,* Oxford University Press, 1985
13. I. Milne, R.A. Ainsworth, A.R. Dowling, and A.T. Stewart, Assessment of the Integrity of Structures Containing Defects, *Int. J. Pressure Vessels Piping,* Vol 32, theme issue, 1988, p 3–104
14. J. Bloom, Appendix J—The Deformation Plasticity Failure Assessment Diagram (DPFAD) Approach to Evaluation of Flaws in Ferritic Piping, presented at the *European Symposium on Elastic-Plastic Fracture Mechanics* (Frieburg, W. Germany) Oct 1989
15. G.G. Chell, A Procedure for Incorporating Thermal and Residual Stresses into the Concept of a Failure Assessment Diagram, *Elastic-Plastic Fracture,* STP 668, ASTM, 1979, p 581–605
16. J.M. Bloom, Prediction of Ductile Tearing Using a Proposed Strain-Hardening Failure Assessment Diagram, *Int. J. Fract.,* Vol 16, 1980, p R73–R77
17. "Standard Test Method for Crack-Tip Opening Displacement (CTOD) Fracture Toughness Assessment," E 1290, *Annual Book of ASTM Standards,* ASTM, 2001
18. "Fracture Mechanics Toughness Tests, Part 1: Method for Determination of K_{Ic}, Critical CTOD and Critical *J* Values of Metallic Materials," BS 5748:1991, British Standards Institution, London, 1991
19. A.G. Miller, Review of Limit Loads of Structures Containing Defects, *Int. J. Pressure Vessels Piping,* Vol 32, theme issue, 1988, p 197–327
20. A.A. Willoughby and T.G. Davy, Plastic Collapse at Part Wall Flaws in Plates, *Fracture Mechanics: Perspectives and Directions,* STP 1020, R.P. Wei, Ed., ASTM, 1989, p 390–409
21. V. Kumar, W.W. Wilkening, W.R. Andrews, M.D. German, H.G. deLorenzi, and D.F. Mowbray, "Estimation Technique for the Prediction of Elastic-Plastic Fracture of Structural Components of Nuclear Systems," 5th and 6th Semiannual Report to EPRI, Contract RP1237-1, General Electric Company, Schenectady, NY, 01 Feb 1981–30 Jan 1982
22. V. Kumar, M.D. German, W.W. Wilkening, W.R. Andrews, H.G. deLorenzi, and D.F. Mowbray, "Advances in Elastic-Plastic Fracture Analysis," EPRI NP-1931, Research Project 1237-1, General Electric Company, Research and Development Center, Schenectady, NY, August 1984
23. V. Kumar and M.D. German, "Further Developments in Elastic-Plastic Fracture Analysis of Through-Wall Flaws and Surface Flaws in Cylinders," Final Report 87-SED-017, Research Project 1237-5, General Electric Company, Research and Development Center, Schenectady, NY, June 1987
24. EPRI/Novetech, *Ductile Fracture Handbook,* Novetech Corporation, Gaithersburg, MD, Vol 1, 1989; Vol 2, 1990; Vol 3, 1991
25. H.S. Reemsnyder, Structural Integrity Analysis of a Heavy Rolled Structural Section, presented at *IIW Conference on Fitness for Purpose of Welded Structures,* International Institute of Welding (Key Biscayne, FL), Oct 1991